THE JOURNAL OF PHYSICAL CHEMISTRY B

Article

pubs.acs.org/JPCB

Modeling the Solubility of Carbon Dioxide in Imidazolium-Based Ionic Liquids with the PC-SAFT Equation of State

Yushu Chen, Fabrice Mutelet,* and Jean-Noël Jaubert

Ecole Nationale Supérieure des Industries Chimiques, Laboratoire Réactions et Génie des Procédés, Université de Lorraine (UPR CNRS 3349), 1 rue Grandville, 54000 Nancy, France

ABSTRACT: The goal of this work was to check the ability of the PC-SAFT equation to represent the solubility of carbon dioxide (CO_2) in ionic liquids. Parameters of pure imidazolium-based ionic liquids were estimated using experimental densities over a large range of temperatures and then correlated with respect to the molecular weight and structure of the solvents. It was found that such a correlation is able to predict the density with high accuracy. The solubility of carbon dioxide in such ionic liquids was then studied. The binary interaction parameter k_{ij} needed for the representation of such binary systems was first fitted to experimental liquid−vapor equilibria data. In a second step, a correlation based on the group contribution concept was developed to determine this temperature-dependent parameter. The ability of the model to describe accurately carbon dioxide solubility in imidazolium-based ionic liquids is demonstrated.

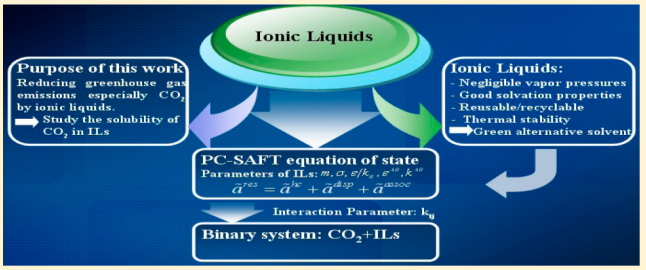

INTRODUCTION

Recent concerns over global warming due to greenhouse gas emissions from fossil fuel combustion have led to the development technologies to reduce and capture these gases. The main greenhouse gases in Earth's atmosphere are water vapor, carbon dioxide (CO_2), methane (CH_4), and nitrous oxide (N_2O). Currently, particular attention is devoted to the CO_2 emissions reductions. There are a number of different separation technologies that can be applied to carbon dioxide capture including solvent-, membrane-, and adsorbent-based processes.

One approach being considered for capturing CO_2 is the use of liquid absorbents designed to selectively solvate CO_2.[1] Alkanolamines are the most generally accepted and widely used of the various available solvents for the removal of CO_2 from natural gas streams. The reactivity and availability at low cost of this family of compounds, especially monoethanolamine and diethanolamine, have allowed these solvents to achieve a pinnacle position in the gas processing industry. Although aqueous alkanolamine solutions are industrially effective for CO_2 removal, this method presents several drawbacks such as intensive energy consumption, high costs, significant losses of alkanolamines within relatively high vapor pressures, and especially corrosion problems in the presence of high-concentration acid gases.[2,3]

Another class of solvents called ionic liquids[4] (ILs) seems to provide good candidates for capturing greenhouse gases because they have some advantages in comparison to other solvents. Indeed, these compounds have good thermal stability and negligible vapor pressure, and they are liquid over a large range of temperatures. Furthermore, the physical properties of ILs can be modified and adjusted by employing different cation−anion combinations.[5−8] Their use and application in industrial processes is somewhat limited for numerous reasons. The thermodynamic properties of pure ionic liquids or dissolved in solution are not always available in the literature. Although numerous thermodynamic models have been evaluated for mixtures containing ionic liquids, no model is purely predictive.

The other background of this work is that the prediction or correlation of thermodynamic characteristics and phase equilibrium with equations of state remains an important goal in chemical and related industries. The use of equations of state has long been restricted to systems of simple fluids; however, there is an increasing demand for models that are also suitable for even more complex fluids. Clearly, some early models derived from statistical mechanics were nonmolecularly based equations of state and were suitable only for simple fluids. During the past few years, many studies have assumed nonspherical molecules to be chains of freely jointed spherical segments. Despite its simplicity, this molecular model accounts for size and shape effects of molecules and has been successfully applied to simple species as well as large polymeric fluids and their mixtures.

A more recent molecularly based equation-of-state concept for chain molecules based on Wertheim's thermodynamic perturbation theory of first order[9−12] was proposed by Chapman et al.[13,14] The essence of this approach, referred to as statistical associating fluid theory (SAFT), is to use a reference fluid that incorporates both the chain length (molecular size and shape) and molecular association, in place of the much simpler hard-sphere reference fluid used in most existing engineering equations of state. The advantage of these molecularly based equations of state is that they not only provide a useful thermodynamic basis for deriving chemical potentials or fugacities that are needed for phase equilibrium simulations but also allow for separating and

Received: July 16, 2012
Revised: November 6, 2012
Published: November 6, 2012

   dx.doi.org/10.1021/jp309944t | J. Phys. Chem. B 2012, 116, 14375−14388

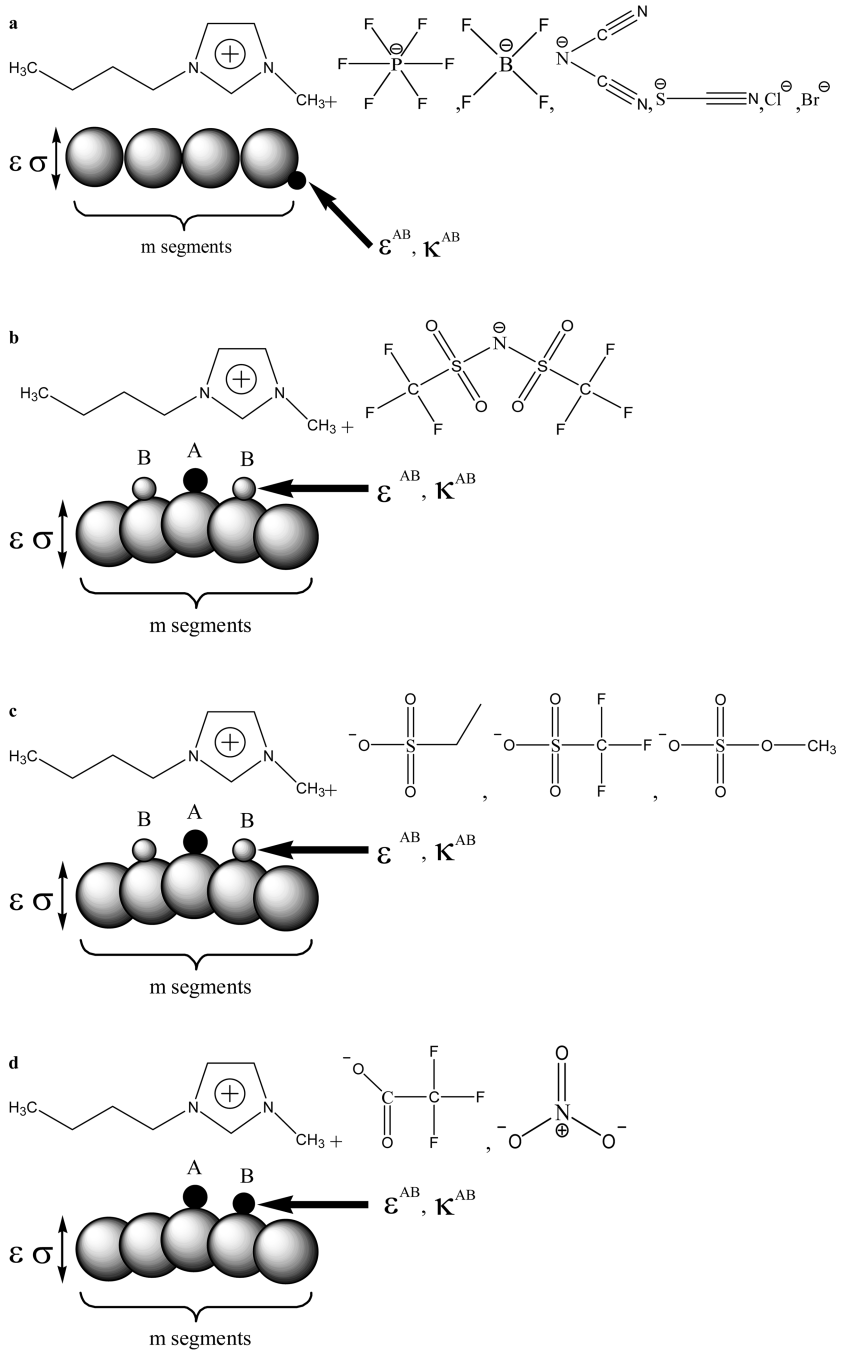

Figure 1. Sketches of the model used to describe the ILs (a) [C_n-mim][BF_4], [C_n-mim][PF_6], [C_n-mim][SCN], [C_n-mim][Cl], [C_n-mim][Br], and [C_n-mim][DCA]; (b) [C_n-mim][Tf_2N]; (c) [C_n-mim][C_2SO_4], [C_n-mim][CF_3SO_3], and [C_n-mim][C_1SO_4]; and (d) [C_n-mim][TFA] and [C_n-mim][NO_3] within the PC-SAFT approach.

quantifying the effects of molecular structure and interactions on bulk properties and phase behavior.

Earlier works related to SAFT focused on the application of the equation to experimental systems[15] or the simplification of the equation to make it more tractable.[16,17] These simplifying versions allow for straightforward calculations and programming, but at the price of a poorer description of the experimental systems of interest. In the late 1990s, many studies and efforts were directed toward refining the equation, especially improving the accuracy of the term used for the reference fluid, despite the more complex mathematical form. This led to different versions of the equation with different acronyms, such as SAFT-VR (for potentials of variable attractive range),[18] soft-SAFT (built from a reference Lennard-Jones fluid),[19,20] and later PC-SAFT (perturbed-chain SAFT).[21]

Recently, Llovell et al.[22] used the soft-SAFT equation to estimate the thermodynamic properties of pure ILs and mixtures containing ILs. The model was used in a predictive manner to check the pability of soft-SAFT to capture the thermodynamic behavior of several complex associating mixtures

dx.doi.org/10.1021/jp309944t | J. Phys. Chem. B 2012, 116, 14375−14388

Table 1. Optimized PC-SAFT Parameters of Pure ILs Considered As Nonassociating Compounds

IL[a]	M_w (g·mol^{-1})	σ (Å)	ε/k_B (K)	m	AAD (%)[b]	ref(s) for experimental density data
[C_2-mim][BF_4]	197.97	3.48	354.39	5.45	0.5190	40−47
[C_4-mim][BF_4]	226.03	3.62	369	6	0.4047	34, 40, 42, 43, 45, 48−64
[C_8-mim][BF_4]	282.13	3.81	389.4	7.14	0.4535	61, 65−67
[C_4-mim][PF_6]	284.18	3.71	391.7	6.25	0.3254	42, 43, 48, 49, 53, 54, 57, 59, 63, 67−81
[C_6-mim][PF_6]	312.24	3.81	395.6	6.74	0.3387	42, 66, 76, 82−86
[C_8-mim][PF_6]	340.29	3.91	395.5	7.14	0.4400	42, 65−67, 75−77, 85−87
[C_2-mim][Tf_2N]	391.32	3.71	390.60	7.83	0.4246	45, 51, 53, 54, 74, 88−93
[C_3-mim][Tf_2N]	405.33	3.76	391.34	8.04	0.5998	88, 94
[C_4-mim][Tf_2N]	419.37	3.81	393.80	8.23	0.2880	51, 53, 54, 73, 74, 84, 88−91, 93, 95, 96
[C_5-mim][Tf_2N]	433.35	3.85	393.50	8.42	0.2994	88, 95
[C_6-mim][Tf_2N]	447.36	3.90	395.00	8.59	0.1370	54, 82, 88, 90, 97−102
[C_7-mim][Tf_2N]	461.45	3.94	395.48	8.81	0.3824	88, 92
[C_8-mim][Tf_2N]	475.48	3.97	396.40	9.00	0.2861	54, 88, 90, 92, 97, 103, 104
[C_2-mim][SCN]	169.25	3.48	346.7	5.3	0.5515	105
[C_4-mim][SCN]	197.3	3.68	356	5.5	0.4268	50, 61, 106, 107
[C_2-mim][CF_3SO_3]	260.24	3.61	390	6.15	0.3065	58, 108−112
[C_4-mim][CF_3SO_3]	288.29	3.82	392.3	6.1	0.3098	51, 54, 62, 63, 66, 80, 109, 113
[C_6-mim][CF_3SO_3]	316.34	3.81	390.5	7.14	0.2691	114, 115
[C_8-mim][CF_3SO_3]	345.41	3.91	398.9	7.54	0.2190	115
[C_4-mim][NO_3]	201.23	3.59	365.8	5.65	0.3705	42, 116, 117
[C_2-mim][TFA]	224.18	3.51	386	6.15	0.3136	112
[C_4-mim][TFA]	252.24	3.71	414	6.34	0.1162	54, 80
[C_2-mim][DCA]	177.21	3.7	364	4.7	0.3825	45, 111, 118
[C_4-mim][DCA]	205.26	3.72	383.4	5.7	0.3764	51, 61, 118−120
[C_6-mim][DCA]	233.31	3.82	404	6.3	0.2212	120
[C_4-mim][C_1SO_4]	250.32	3.61	376.9	6.74	0.2612	43, 58, 61, 63, 76, 109, 121−125
[C_2-mim][C_2SO_4]	236.29	3.71	384	5.66	0.6024	53, 58, 74, 89, 93, 96, 111, 112, 117, 125−132
[C_4-mim][Cl]	174.67	3.49	359	5.66	1.0250	133−135
[C_6-mim][Cl]	202.37	3.7	366.4	5.8	0.4177	42, 126, 135, 136
[C_8-mim][Cl]	230.78	3.92	391.9	5.81	0.3476	42, 135−138
[C_2-mim][AC]	170.21	3.48	364.5	5.5	0.4571	105, 139, 140
[C_4-mim][AC]	198.27	3.72	378	5.51	0.3299	141, 142
[C_6-mim][Br]	247.18	3.61	374	6.54	0.2175	143
CO_2	44.01	2.0729	169.21	2.7852	0	21

[a] For the [C_n-mim][Tf_2N] family, parameters for the members with n = 2, 4, 6, and 8 were obtained by fitting to experimental data, and parameters corresponding to n = 3, 5, and 7 were obtained using the correlations presented in eq 23. [b]

$$\text{AAD (\%)} = \frac{100}{n_{pts}} \sum_{i=1}^{n_{pts}} \left| \frac{\rho_i^{sat,exp} - \rho_i^{sat,cal}}{\rho_i^{sat,exp}} \right|$$

such as the behavior of binary mixtures of ionic liquids with different cations and anions, the vapor−liquid equilibria (VLE) of mixtures containing short-chain alcohols and dialkylimidazolium [Tf_2N], and the liquid−liquid equilibria of {water + IL} binary systems. They showed that such phase equilibria could be represented with high accuracy using soft-SAFT.

The truncated perturbed-chain polar statistical associating fluid theory (tPC-PSAFT)[23,24] was also evaluated for the prediction of CO_2 solubility in dialkylimidazolium ionic liquids. In their works, Kroon et al.[25] and Karakatsani et al.[26] calculated the parameters of pure ionic liquids by fitting them to experimental liquid density data. In the case of pure ILs, the association contribution was not taken into account, but dipolar interactions of IL molecules and quadrupolar interactions of CO_2 molecules were considered. For ILs, they assumed that the polarity was comparable to the polarity of lower to medium alcohols.

Then, Domanska et al.[27] proposed to represent the liquid−liquid equilibria of binary systems containing aliphatic hydrocarbons and piperidinium-based ionic liquids by the perturbed-chain SAFT (PC-SAFT) equation and the nonrandom hydrogen-bonding (NRHB) theory. Pure-fluid parameters of the model were obtained from experimental liquid density and solubility parameter data at ambient pressure and tested against high-pressure densities. The authors showed that the PC-SAFT and NRHB models were both able to capture phase behavior in a qualitative manner.

In this work, the PC-SAFT equation of state (EoS) was chosen to model both the pure components and the binary systems {CO_2 + IL}. Indeed, a theory such as PC-SAFT that is a molecularly based equation of state offers several advantages. The first advantage is that each of the approximations made in the development of SAFT such as the chain, association, and polar terms has been verified against molecular simulation results. In this way, the range of applicability and the shortcomings of each term in the equation of state have been assessed. A second advantage is that the SAFT parameters have physical meaning, which can help in checking the accuracy

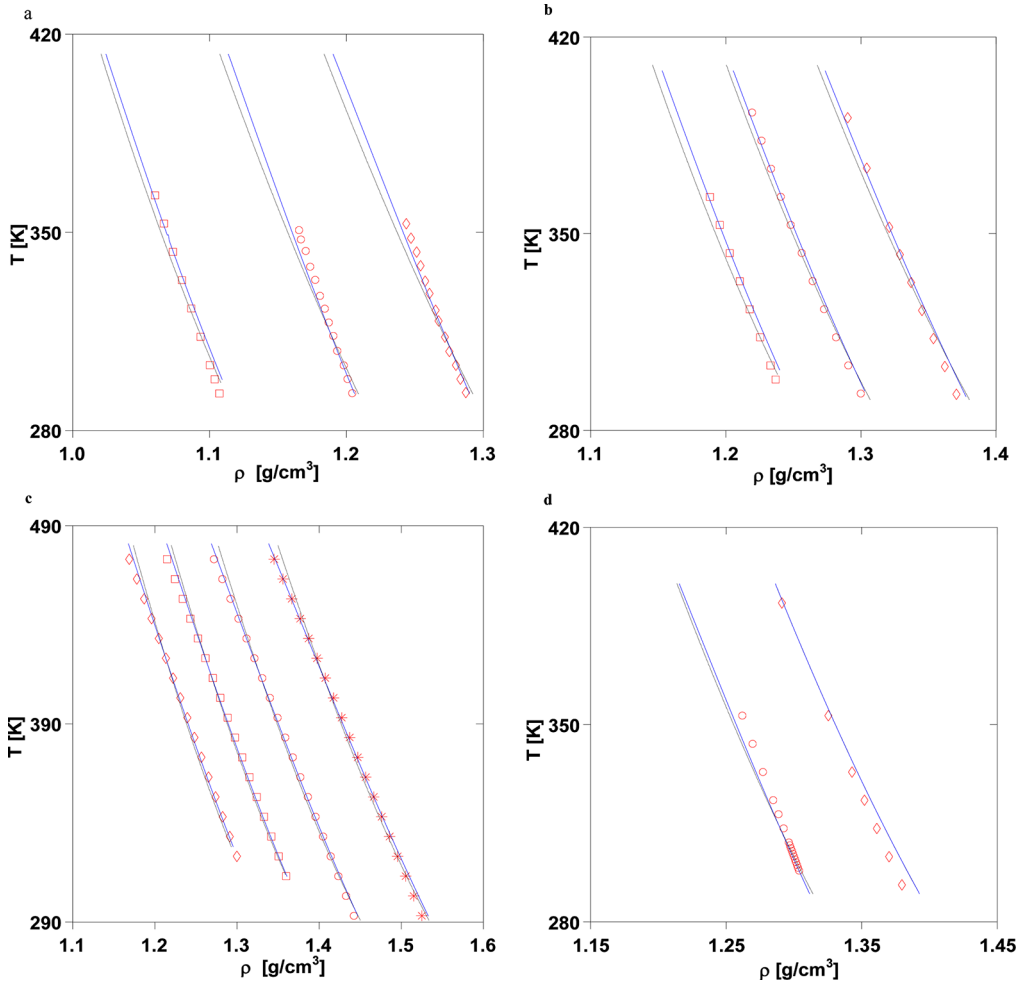

Figure 2. Temperature−density diagrams for ILs considered as nonassociating and self-associating compounds. Symbols, experimental data used in the parameter estimation; solid lines, self-associating estimations; dotted lines, nonassociating estimations. (a) $[C_2\text{-mim}][BF_4]$ (◊), $[C_4\text{-mim}][BF_4]$ (○), and $[C_8\text{-mim}][BF_4]$ (□); (b) $[C_4\text{-mim}][PF_6]$ (◊), $[C_6\text{-mim}][PF_6]$ (○), and $[C_8\text{-mim}][PF_6]$ (□); (c) $[C_2\text{-mim}][Tf_2N]$ (*), $[C_4\text{-mim}][Tf_2N]$ (○), $[C_6\text{-mim}][Tf_2N]$ (□), and $[C_8\text{-mim}][Tf_2N]$ (◊); and (d) $[C_2\text{-mim}][CF_3SO_3]$ (◊) and $[C_4\text{-mim}][CF_3SO_3]$ (○).

and correctness of the parameters during modeling of the pure components. A third advantage is that, as for all molecularly based equations of state, PC-SAFT is a useful tool in which the effects of molecular structure on the thermodynamic properties can be separated and quantified.

PC-SAFT Modeling. The pertubed-chain statistical associating fluid theory (PC-SAFT) EoS, which is similar to other SAFT-type equations of state, was developed in 2001 by Gross and Sadowski.[21] Applying a perturbation theory for chain molecules inspired by two articles by Barker and Henderson,[28,29] Gross and Sadowski derived a dispersion expression for chain molecules and used a hard-chain reference fluid, for comparison with other classical SAFT equations of state that used a hard-sphere reference, meaning that the dispersion term accounts for attractions between spherical segments not attractions between hard chains.

The PC-SAFT equation is usually written in terms of the residual Helmholtz free energy. Each term in the equation represents a different microscopic contribution to the total free energy of the fluid. The equation is given by

$$\tilde{a}^{\mathrm{res}} = \tilde{a}^{\mathrm{hc}} + \tilde{a}^{\mathrm{disp}} + \tilde{a}^{\mathrm{assoc}} \tag{1}$$

where $\tilde{a}^{\mathrm{res}}$ is the residual Helmholtz free energy of the system ($\tilde{a}^{\mathrm{res}} = \tilde{a}^{\mathrm{total}} - \tilde{a}^{\mathrm{ideal}}$). The superscripts hc, disp, and assoc refer to a reference hard-chain contribution, a dispersion contribution, and an associating contribution, respectively, where $\tilde{a} = a/RT$.

The hard-sphere chain contribution was provided and defined by Gross and Sadowski[21] as

$$\tilde{a}^{\mathrm{hc}} = \bar{m}\tilde{a}^{\mathrm{hs}} - \sum_{i=1}^{n_c} x_i(m_i - 1)\ln g_{ij}^{\mathrm{hs}} \tag{2}$$

It depends on the radial pair distribution function for segments in the hard-sphere system (g_{ij}^{hs}), the hard-sphere contribution ($\tilde{a}^{\mathrm{hs}}$), and the mean segment number ($\bar{m}$), which is a function of m, the number of segments per chain.

The radial pair distribution function (g_{ij}^{hs}) and the hard-sphere contribution ($\tilde{a}^{\mathrm{hs}}$) are defined as

$$g_{ij}^{\mathrm{hs}} = \frac{1}{1-\zeta_3} + d_{ij}\frac{3\zeta_2}{(1-\zeta_3)^2} + d_{ij}^2\frac{2\zeta_2^2}{(1-\zeta_3)^3}, \quad \{i,j\} \in [1, n_c]^2 \tag{3}$$

$$\tilde{a}^{\mathrm{hs}} = \frac{1}{\zeta_0}\left[\frac{3\zeta_1\zeta_2}{1-\zeta_3} + \frac{\zeta_2^3}{\zeta_3(1-\zeta_3)^2} + \left(\frac{\zeta_2^3}{\zeta_3^2} - \zeta_0\right)\ln(1-\zeta_3)\right] \tag{4}$$

where d_i and ζ_n are given by

dx.doi.org/10.1021/jp309944t | J. Phys. Chem. B 2012, 116, 14375−14388

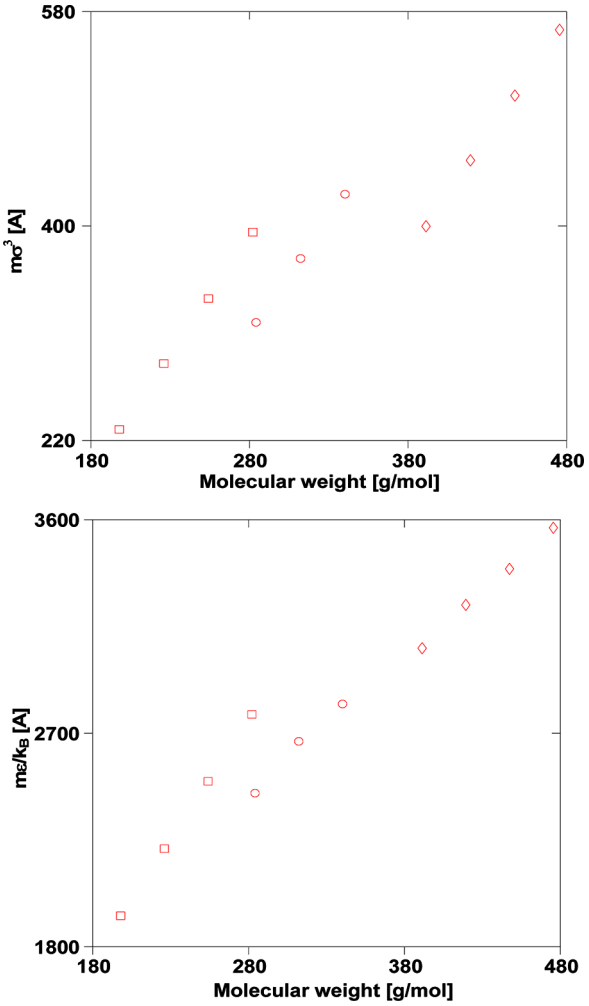

Figure 3. Pure-component parameters $m\sigma^3$ and $m\varepsilon/k_B$ of the PC-SAFT EoS for the $[C_n\text{-mim}][Tf_2N]$ (◊), $[C_n\text{-mim}][BF_4]$ (□), and $[C_n\text{-mim}][PF_6]$ (○) families as functions of IL molecular weight.

$$d_i(T) = \sigma_i\left[1 - 0.12\exp\left(-\frac{3\varepsilon_i}{k_B T}\right)\right], \quad i \in [1, n_c] \tag{5}$$

$$d_{ij} = \frac{d_i d_j}{d_i + d_j} \tag{6}$$

$$\zeta_n = \frac{\pi}{6}\tilde{\rho}\sum_{i=1}^{n_c} x_i m_i d_i^{\,n}, \quad n \in [0, 3] \tag{7}$$

The dispersion contribution to the Helmholtz free energy, $\tilde{a}^{disp}$, accounts for van der Waals forces. In this work, we use the dispersion expression defined by Gross and Sadowski[21]

$$\tilde{a}^{disp} = -2\pi\tilde{\rho}I_1\overline{m^2\varepsilon\sigma^3} - \pi\tilde{\rho}\bar{m}C_1 I_2\overline{m^2\varepsilon^2\sigma^3} \tag{8}$$

where the coefficient C_1 depends on the mean segment number $(\bar{m})$ and the reduced density η, defined by $\eta = \zeta_3$

$$C_1 = \left[1 + \bar{m}\frac{8\eta - 2\eta^2}{(1-\eta)^4} + (1-\bar{m})\frac{20\eta - 27\eta^2 + 12\eta^3 - 2\eta^4}{[(1-\eta)(2-\eta)]^2}\right]^{-1} \tag{9}$$

I_1 and I_2 are expressed as

$$I_1 = \sum_{i=0}^{6} a_i\eta^i \tag{10}$$

$$I_2 = \sum_{i=0}^{6} b_i\eta^i \tag{11}$$

where the quantities $\overline{m^2\varepsilon\sigma^3}$ and $\overline{m^2\varepsilon^2\sigma^3}$ are defined as

$$\overline{m^2\varepsilon\sigma^3} = \sum_{i=1}^{n_c}\sum_{j=1}^{n_c} x_i x_j m_i m_j\left(\frac{\varepsilon_{ij}}{k_B T}\right)\sigma_{ij}^{\,3} \tag{12}$$

$$\overline{m^2\varepsilon^2\sigma^3} = \sum_{i=1}^{n_c}\sum_{j=1}^{n_c} x_i x_j m_i m_j\left(\frac{\varepsilon_{ij}}{k_B T}\right)^2\sigma_{ij}^{\,3} \tag{13}$$

Conventional combining rules for ε_{ij} and σ_{ij} were employed

$$\sigma_{ij} = \frac{\sigma_i + \sigma_j}{2} \tag{14}$$

$$\varepsilon_{ij} = \sqrt{\varepsilon_i\varepsilon_j}(1 - k_{ij}) \tag{15}$$

where k_{ij} is the binary interaction parameter.

For evaluating the VLE of normal fluids, inclusion of $\tilde{a}^{hc}$ and $\tilde{a}^{disp}$ in the PC-SAFT approach is sufficient. Three parameters, the segment number (m), the segment energy parameter (ε/k_B), and the segment diameter (σ) are required to characterize each compound. However, in alkanol or acid solution, hydrogen bonding contributes dominantly to the nonideality of these solutions, and its contribution should be taken into account. The Helmholtz free energy due to association $\tilde{a}^{assoc}$ is defined as[15,30]

$$\tilde{a}^{assoc} = \sum_{i=1}^{n_c} x_i\left[\sum_{A_i}\left(\ln X^{A_i} - \frac{X^{A_i}}{2}\right) + \frac{1}{2}M_i\right] \tag{16}$$

where X^{A_i} is the mole fraction of molecules i not bonded at site A, M_i is the number of association sites on each molecule, and $\sum_{A_i}$ represents a sum over all associating sites on each molecule. The parameter X^{A_i} is given by

$$X^{A_i} = [1 + N_{AV}\sum_j\sum_{B_j}\rho_j X^{B_j}\Delta^{A_iB_j}]^{-1} \tag{17}$$

where the internal summation sign runs over all sites on molecule j. ρ_j is the molar density of component j

$$\rho_j = x_j\rho \tag{18}$$

The association strength $\Delta^{A_iB_j}$ is given by

$$\Delta^{A_iB_j} = g_{ij}^{hs}[\exp(\varepsilon^{A_iB_j}/k_B T) - 1](\sigma_{ij}^{\,3}k^{A_iB_j}) \tag{19}$$

and depends on the association energy $\varepsilon^{A_iB_j}$ and the association volume $k^{A_iB_j}$ between associating substances i and j. The combining rules suggested by Wolbach and Sandler,[31] namely

$$\varepsilon^{A_iB_j} = \frac{1}{2}(\varepsilon^{A_iB_i} + \varepsilon^{A_jB_j}) \tag{20}$$

dx.doi.org/10.1021/jp309944t | J. Phys. Chem. B 2012, 116, 14375−14388

Table 2. Optimized PC-SAFT Parameters of Pure ILs Considered As Self-Associating Molecules

IL	M_w (g·mol^{-1})	σ (Å)	ε/k_B (K)	m	K_{AB}	ε_{AB}/k_B (K)	AAD (%)
[C_2-mim][BF_4]	197.97	4.23	408.1	3.13	0.00225	3450	0.2315
[C_4-mim][BF_4]	226.03	4.33	426.7	3.62	0.00225	3450	0.3019
[C_8-mim][BF_4]	282.13	4.32	434	5.03	0.00225	3450	0.1263
[C_4-mim][PF_6]	284.18	4.23	421	4.3	0.00225	3450	0.1870
[C_6-mim][PF_6]	312.24	4.32	431.8	4.73	0.00225	3450	0.1666
[C_8-mim][PF_6]	340.29	4.32	433.8	5.42	0.00225	3450	0.1430
[C_2-mim][Tf_2N]	391.32	4.18	360.5	5.38	0.00225	3450	0.1346
[C_3-mim][Tf_2N]	405.33	4.20	368.48	5.68	0.00225	3450	0.5014
[C_4-mim][Tf_2N]	419.37	4.21	375.2	6.05	0.00225	3450	0.1213
[C_5-mim][Tf_2N]	433.35	4.26	377.85	6.19	0.00225	3450	0.1599
[C_6-mim][Tf_2N]	447.36	4.31	385.2	6.35	0.00225	3450	0.1343
[C_7-mim][Tf_2N]	461.45	4.31	385.80	6.71	0.00225	3450	0.1731
[C_8-mim][Tf_2N]	475.48	4.32	386.9	7	0.00225	3450	0.1907
[C_2-mim][SCN]	169.25	4.22	383.8	3.05	0.00225	3450	0.3247
[C_4-mim][SCN]	197.3	4.21	383.5	3.77	0.00225	3450	0.2497
[C_2-mim][CF_3SO_3]	260.24	4.27	373.9	3.68	0.00225	3450	0.3165
[C_4-mim][CF_3SO_3]	288.29	4.43	392	3.92	0.00225	3450	0.2352
[C_6-mim][CF_3SO_3]	316.34	4.32	397.9	4.93	0.00225	3450	0.2374
[C_8-mim][CF_3SO_3]	345.41	4.41	398.1	5.26	0.00225	3450	0.2038
[C_4-mim][NO_3]	201.23	4.23	393.7	3.52	0.00225	3450	0.2417
[C_2-mim][TFA]	224.18	4.230	395.80	3.520	0.00225	3450	0.1636
[C_4-mim][TFA]	252.24	4.430	417.00	3.710	0.00225	3450	0.0627
[C_2-mim][DCA]	177.21	4.340	409.40	3.010	0.00225	3450	0.3855
[C_4-mim][DCA]	205.26	4.440	411.10	3.400	0.00225	3450	0.2102
[C_6-mim][DCA]	233.31	4.53	429.2	3.82	0.00225	3450	0.1173
[C_4-mim][C_1SO_4]	250.32	4.43	422.9	3.72	0.00225	3450	0.1682
[C_2-mim][C_2SO_4]	236.29	4.22	419	3.94	0.00225	3450	0.5331
[C_4-mim][Cl]	174.67	4.130	402.60	3.520	0.00225	3450	0.8482
[C_6-mim][Cl]	202.37	4.33	407.8	3.72	0.00225	3450	0.3351
[C_8-mim][Cl]	230.78	4.53	413.8	3.82	0.00225	3450	0.2506
[C_2-mim][AC]	170.21	4.23	405.70	3.130	0.00225	3450	0.3078
[C_4-mim][AC]	198.27	4.43	414	3.33	0.00225	3450	0.2402
[C_6-mim][Br]	247.18	4.210	391.90	4.170	0.00225	3450	0.1660
CO_2	44.01	2.0729	169.21	2.7852	0	0	0

$$k^{A_iB_j} = \sqrt{k^{A_iB_i}k^{A_jB_j}}\left(\frac{\sqrt{\sigma_{ii}\sigma_{jj}}}{0.5(\sigma_{ii}+\sigma_{jj})}\right)^3 \quad (21)$$

were used. Hence, if one of the substances in a mixture is nonassociating, $k^{A_iB_j}$ and $\Delta^{A_iB_j}$ will vanish.

Molecular Model for Carbon Dioxide and ILs. Following the approach of Huang and Radoz,[15] the carbon dioxide molecule was modeled as a nonassociating substance. This molecule was thus represented by three molecular parameters: m, the segment number; σ, the segment diameter; and ε/k_B, the segment energy parameter. The values used were taken from the article by Gross and Sadowski.[21]

In this work, the PC-SAFT parameters of pure ILs were first determined by considering the ILs as nonassociating compounds. The three pure-component parameters (m, σ, ε/k_B) were obtained by fitting pure-component data. In a second step, the ILs were considered as self-associating molecules. However, to keep a minimum number of parameters to be fitted, the associating parameters ($\varepsilon^{A_iB_j}$ and $k^{A_iB_j}$) were transferred from those of 1-alkanols,[32] that is, $\varepsilon^{A_iB_j}$ = 3450 K and $k^{A_iB_j}$ = 0.00225. Both associating parameters were assumed to be constant for the whole IL family because the alkyl chain length of the cation does not affect the strength of the associating bonds. These two sets of parameters were compared to determine whether the associating contribution of ILs should be taken into account.

We focused on the most frequently studied imidazolium-based ILs. These ILs are 1-alkyl-3-methylimidazolium tetrafluoroborate, [C_n-mim][BF_4]; 1-alkyl-3-methylimidazolium hexafluoroborate, [C_n-mim][PF_6]; 1-alkyl-3-methylimidazolium bistrifluoromethylsulfonylimide, [C_n-mim][Tf_2N]; 1-alkyl-3-methylimidazolium thiocyanate, [C_n-mim][SCN]; 1-alkyl-3-methylimidazolium ethylsulfate, [C_n-mim][C_2SO_4]; 1-alkyl-3-methylimidazolium trifluoromethanesulfonate, [C_n-mim][CF_3SO_3]; 1-alkyl-3-methylimidazolium dicyanmide, [C_n-mim][DCA]; 1-alkyl-3-methylimidazolium trifluoroacetate, [C_n-mim][TFA]; 1-alkyl-3-methylimidazolium nitrate, [C_n-mim][NO_3]; 1-alkyl-3-methylimidazolium methylsulfate, [C_n-mim][C_1SO_4]; 1-alkyl-3-methylimidazolium chloride, [C_n-mim][Cl]; 1-alkyl-3-methylimidazolium bromide, [C_n-mim][Br]; and 1-alkyl-3-methylimidazolium acetate, [C_n-mim][AC].

Following the studies performed by Llovell et al.,[22] Andreu and Vega,[33] and Huang and Radosz,[15] the ILs of the families [C_n-mim][BF_4], [C_n-mim][PF_6], [C_n-mim][SCN], [C_n-mim]-[Cl], [C_n-mim][Br], and [C_n-mim][DCA] were modeled as Lennard-Jones chains with one associating site in each molecule (Figure 1a). This model thus considers the neutral pairs composed by the anion and the cation as a single chain molecule with this association site describing the specific interactions. For the [C_n-mim][Tf_2N] family, the ILs were modeled as homonuclear chainlike molecules with three associating sites mimicking the strong interactions between the anion and the cation (Figure 1b).

dx.doi.org/10.1021/jp309944t | J. Phys. Chem. B 2012, 116, 14375−14388

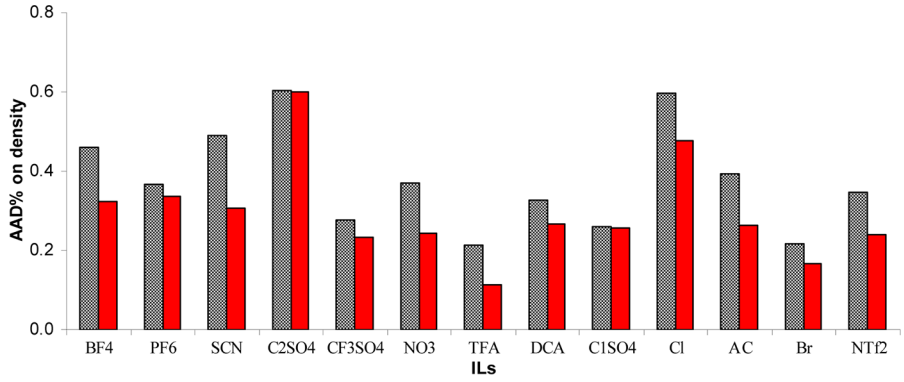

Figure 4. Average absolute deviations of density for different families of ILs. Black rectangles, ILs considered as nonassociating compounds; red rectangles, ILs considered as associating compounds.

Table 3. Parameters Used in Eq 24 to Estimate m, σ, and ε/k_B for the $[C_n\text{-mim}]$ Families of ILs

IL family	a_i	b_i	c_i	d_i	e_i	f_i
$[C_n\text{-mim}][BF_4]$	0.0224	−1.3539	2.0042	−159.6301	10.7046	−852.1832
$[C_n\text{-mim}][PF_6]$	0.0196	−1.3030	1.9890	−239.7743	9.4840	−893.8708
$[C_n\text{-mim}][SCN]$	0.0257	−1.2944	1.8592	−85.4749	9.7487	−478.6220
$[C_n\text{-mim}][CF_3SO_3]$	0.0200	−1.6170	1.9473	−220.2002	9.0532	−1001.8402
$[C_n\text{-mim}][TFA]$	0.0068	2.0020	1.9895	−179.4601	5.5205	155.1283
$[C_n\text{-mim}][DCA]$	0.0144	0.4550	1.9327	−97.1372	7.1208	−39.0765
$[C_n\text{-mim}][Cl]$	0.0054	2.5946	1.9157	−86.4376	2.9395	909.3006
$[C_n\text{-mim}][AC]$	0.0071	1.9168	1.8752	−82.2877	3.9254	601.0192
$[C_n\text{-mim}][Tf_2N]$	0.0184	−1.7982	2.0398	−404.7292	8.9773	−1549.9298

The number of associating sites was chosen on the basis of the delocalization of the anion electric charge due to the oxygen groups, enhancing the possibility of interaction with the surrounding cations through them. As a consequence, one associating A-type site represents the nitrogen atom interaction with the cation, whereas two B sites represent the delocalized charge due to the oxygen atoms on the anion, allowing only AB interactions between different IL molecules. For the $[C_n\text{-mim}][C_2SO_4]$, $[C_n\text{-mim}][CF_3SO_3]$, and the $[C_n\text{-mim}][C_1SO_4]$ families, the ILs were modeled as chainlike molecules with three associating sites between the anion and the cation (Figure 1c): one associating A-type site represents the oxygen atom interaction with the cation, and two B sites represent the delocalized charge due to the oxygen atoms on the anion. For the $[C_n\text{-mim}][TFA]$ and $[C_n\text{-mim}][NO_3]$ families, the ILs were modeled as chain molecules with two associating sites (Figure 1d): one associating A-type site represents the oxygen atom interaction with cation, and one associating B-type site represents the oxygen atom on the anion interacting with the cation.

RESULTS AND DISCUSSION

Pure Components. The PC-SAFT equation was evaluated in the representation of the thermodynamic properties of pure ILs such as temperature-dependent density. ILs were considered both as self-associating and nonassociating molecules. The set of PC-SAFT parameters for carbon dioxide was taken from the literature and is presented in Table 1.[21] The parameters m, σ, and ε/k_B of the ILs were determined to minimize the following objective function (OF)

$$\mathrm{OF} = \sum_{i=1}^{n_{pts}} \left(\frac{\rho_i^{sat,exp} - \rho_i^{sat,cal}}{\rho_i^{sat,exp}} \right)^2 \quad (22)$$

which takes into account the deviations between calculated (cal) and experimental (exp) liquid densities.

ILs as Nonassociating Compounds. In the first step, the ILs were considered as nonassociating compounds. Parameters m, σ, and ε/k_B obtained after optimization for the ILs studied in this work are provided in Table 1. The resulting density−temperature diagrams are shown in Figure 2a for the $[C_n\text{-mim}][BF_4]$ family, Figure 2b for the $[C_n\text{-mim}][PF_6]$ family, Figure 2c for the $[C_n\text{-mim}][Tf_2N]$ family, and Figure 2d for the $[C_n\text{-mim}][CF_3SO_3]$ family. The average absolute deviation (AAD, %) of the density for all of the ILs considered in this work is about 0.38%. We can thus conclude that the density is globally well correlated even if deviations are observed at high and low temperatures. A linear relationship between the three parameters of the ILs and their molecular weight was observed for each family of ILs studied in this work. As examples, $m\sigma^3$ and $m\varepsilon/k_B$ are depicted as functions of the molecular weight in Figure 3 for the $[C_n\text{-mim}][Tf_2N]$, $[C_n\text{-mim}][BF_4]$, and $[C_n\text{-mim}][PF_6]$ families. The corresponding equations for the $[C_n\text{-mim}][Tf_2N]$-based ILs (with n = 2, 4, 6, and 8) are

$$m = 0.0138M_w + 2.4503$$
$$m\sigma^3 = 1.958M_w - 366.23$$
$$m\varepsilon/k_B = 5.9721M_w + 726.42 \quad (23)$$

These correlations were used to predict the experimental densities of three other ILs not taken into account in the database: $[C_3\text{-mim}][Tf_2N]$, $[C_5\text{-mim}][Tf_2N]$, and $[C_7\text{-mim}][Tf_2N]$. The PC-SAFT parameters of these ILs were calculated using eq 23. Good agreement with the experimental density data is observed, and the results for the AAD (%) of the densities are

dx.doi.org/10.1021/jp309944t | J. Phys. Chem. B 2012, 116, 14375−14388

given in Table 1. Therefore, these correlations are useful because they provide the possibility of predicting the behavior of heavier members of a given family without needing experimental data.

ILs as Self-Associating Compounds. Second, the parameters of the ILs taken as self-associating compounds were estimated. As mentioned before, the association parameters $\varepsilon^{A_iB_j}$ and $k^{A_iB_j}$ were kept constant and equal to those of 1-alkanols.[32] Parameters m, σ, and ε/k_B were estimated by minimizing eq 22. The results for the molecular parameters and average absolute deviation (AAD, %) in the density are provided in Table 2. The AAD in the density for all of the ILs is about 0.29%. The trend of deviations for each family of ILs is shown in Figure 4. The largest deviations were obtained for the $[C_2SO_4]$- and [Cl]-based ILs. There is thus a great improvement by using self-associating parameters. Meanwhile, one can notice this significant improvement through the density−temperature diagrams shown in Figure 2a−d. We can thus conclude that the associating contribution should be taken into account to accurately correlate the properties of ILs.

It was thus decided to develop simple correlations to predict the three molecular parameters m, σ, and ε/k_B of the PC-SAFT model for the different families of ILs. The approach is based on the fact that m, $m\sigma^3$, and $m\varepsilon/k_B$ are each linearly related to the molecular weights of the ILs. The correlations are as follows

$$m = a_i M_w + b_i$$
$$m\sigma^3 = c_i M_w + d_i$$
$$m\varepsilon/k_B = e_i M_w + f_i \quad (24)$$

where a_i, b_i, c_i, d_i, e_i, and f_i are the constants characterizing family i of ILs. In this work, nine families of $[C_n$-mim] ILs were defined depending on the associated anion (BF_4, PF_6, NTF_2, SCN, CF_3SO_3, TFA, DCA, AC, and Cl). Parameters suitable for such correlations are given in Table 3. The average absolute deviation in the density calculated using the parameters estimated from these correlations is equal to 0.29%. Therefore, the densities calculated from these parameters are globally accurate as compared to available experimental data. The approach was also evaluated through a new IL not used to determine the parameters in eq 24, namely, 1-hexyl-3-methylimidazolum tetrafluoroborate.[34] For this IL, the parameters obtained from eq 24 led to AAD = 0.10%, to be compared with AAD = 0.06% calculated by a direct fit of the parameters to the experimental density data. In summary, the PC-SAFT model provides the possibility of predicting the behavior of new members of a given family with the help of the correlations developed in this work.

Moreover, we checked the validity of the adjusted parameters listed in Table 2 to predict the vapor pressures of some ILs and compared the PC-SAFT calculations with available experimental data. Recently, Rocha et al.[144] and Zaitsau et al.[103] measured the vapor pressures of several imidazolium ILs ($[C_n$-mim]-$[NTF_2]$ with n = 2, 4, 6, and 8). The vapor pressure was measured by the integral effusion Knudsen method in the temperature range T = 450−500 K.

Calculated vapor pressures and experimental data are plotted in the Figure 5. The observed deviations from the experimental data are particularly significant. For ILs with short alkyl chains, the predicted vapor pressure is about 4 orders of magnitude higher than the experimental value. The difference between the calculated and experimental vapor pressures decreases as the alkyl chain length increases. It is important to note that calculated vapor pressures of ILs are underestimated when the ILs are taken as nonassociating fluids and overestimated when the ILs are defined as associating fluids. Recently, Llovell et al.[22] presented similar calculations on $[Tf_2N]$-based ILs using the soft-SAFT EoS. The authors obtained overestimated values of vapor pressure for all ILs, and the difference was about 2 orders of magnitude. Similar calculations were proposed by Paduszyński and Domanska[145] using the PC-SAFT model and a 10-site model. The authors concluded that their approach tends to enhance the vapor pressure predictions of ILs. Therefore, we decided to determine the molecular parameters of the PC-SAFT model for the $[C_n$-mim$][Tf_2N]$ family using density and vapor pressure data. The molecular parameters and the average

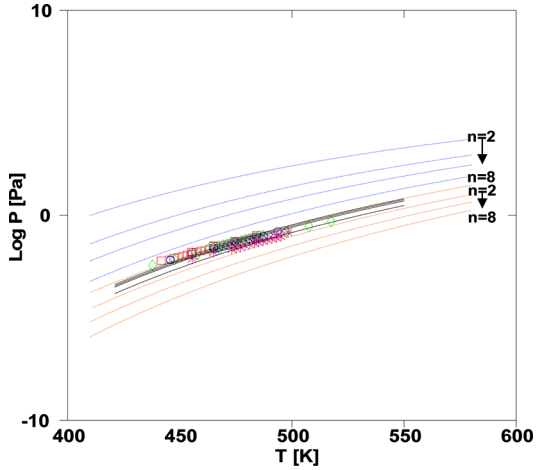

Figure 5. Vapor pressures for $[C_2$-mim$][Tf_2N]$ (□), $[C_4$-mim$][Tf_2N]$ (◊), $[C_6$-mim$][Tf_2N]$ (○), and $[C_8$-mim$][Tf_2N]$ (*). The symbols represent the experimental data. Blue dotted lines, ILs considered as associating compounds using PC-SAFT parameters adjusted on experimental density data only; orange dotted lines, ILs considered as nonassociating compounds using PC-SAFT parameters adjusted on experimental density data only; and black solid lines, ILs considered as associating compounds using PC-SAFT parameters adjusted on experimental pressure and density data.

Table 4. Optimized PC-SAFT Parameters of the Family $[C_n$-mim$][Tf_2N]$ Obtained Using Experimental Density and Pressure Data

IL	M_w (g·mol^{-1})	σ (Å)	ε/k_B (K)	m	K_{AB}	ε_{AB}/k_B (K)	AAD (%) pressure	AAD (%) density
$[C_2$-mim$][Tf_2N]$	391.32	4.28	457.40	5.67	0.00225	3450	11.81	1.28
$[C_4$-mim$][Tf_2N]$	419.37	4.37	458.90	5.72	0.00225	3450	9.41	4.29
$[C_6$-mim$][Tf_2N]$	447.36	4.47	460.30	5.78	0.00225	3450	6.49	1.66
$[C_8$-mim$][Tf_2N]$	475.48	4.63	461.60	5.83	0.00225	3450	5.14	2.89

dx.doi.org/10.1021/jp309944t | J. Phys. Chem. B 2012, 116, 14375−14388

absolute deviations in vapor pressure and density are given in Table 4. In this case, the vapor pressures and densities of [Tf_2N]-based ILs were determined with good accuracy.

Mixtures: Solubility of CO_2 in ILs. The use of the PC-SAFT EoS for mixtures requires knowledge of the binary interaction parameter k_{ij}. Up to now, there is no general correlation to determine this parameter, which is generally fitted on experimental VLE data. Many thermodynamic models can be used in a purely predictive manner by keeping k_{ij} constant (k_{ij} = 0 or 1) such as the soft-SAFT model. However, it was demonstrated that better results are obtained when the interaction parameter is temperature-dependent and different from 0 (or 1). As an example, results for {[C_4-mim][BF_4] + CO_2} at T = 323 K with k_{ij} constant (k_{ij} = 0, 1) and k_{ij} fitted by VLE data are shown in Figure 6. A large difference was found for k_{ij} = 0 or 1 as compared to the experimental data. Therefore, in this work, the k_{ij} parameters of various {IL + CO_2} binary mixtures were determined to minimize the deviations between calculated and experimental VLE data on an extended database. A flash algorithm was used to perform VLE calculations [for a selected binary system and a given T and P, we have found the compositions of the liquid (x) and gas (y) phases in equilibrium]. Values of interaction parameters k_{ij} at different temperatures are reported in Table 5. Figure 7 highlights that k_{ij} is a temperature-dependent parameter and increases linearly with temperature. A model based on the group contribution concept for the determination of the interaction parameter was thus developed. In our approach, each imidazolium-based ionic liquids is characterized by two groups: one group for the anion and another group ($-CH_3$ or $-CH_2-$) to describe the alkyl chain grafted on the cation. This correlation is

$$k_{ij} = (a_i + n a_{CH_3/CH_2})T + (b_i + n b_{CH_3/CH_2}) \quad (25)$$

where a_i and b_i are the contributions of anion i and a_{CH_3/CH_2} and b_{CH_3/CH_2} are used for describing the alkyl chain grafted on the cation, the length of which is characterized by n carbon atoms. The values of all parameters a_i, b_i, a_{CH_3/CH_2}, and b_{CH_3/CH_2} are given in Table 6. Vapor−liquid equilibrium calculations of {CO_2 + ionic liquid} binary systems were performed using the interaction parameters obtained from eq 25. The average

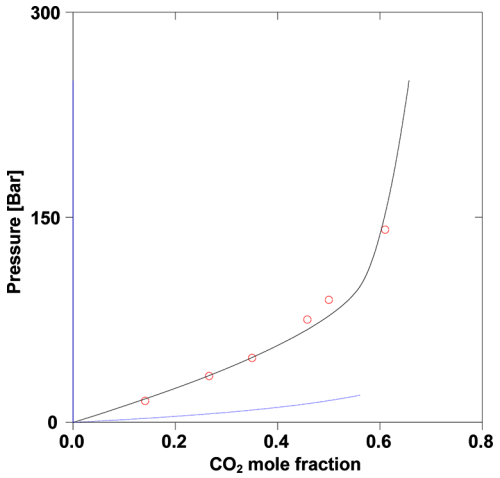

Figure 6. Solubility of CO_2 in [C_4-mim][BF_4] at T = 323 K (○) obtained with different k_{ij} values. Symbols represent experimental data. Blue dotted lines, k_{ij} = 0; blue solid lines, k_{ij} = 1; black solid lines, k_{ij} fitted with experimental data.

Table 5. k_{ij} Interaction Parameters at Different Temperatures for CO_2 + IL Binary Mixtures

		A[a]		B[b]				A[a]		B[b]	
IL	T (K)	k_{ij}	AAD[c] (%)	k_{ij}	AAD[c] (%)	IL	T (K)	k_{ij}	AAD[c] (%)	k_{ij}	AAD[c] (%)
[C_2-mim][BF_4]	298.20	0.159	2.516	0.1588	2.521	[C_2-mim][Tf_2N]	303.85	0.089	4.418	0.0949	5.845
	313.20	0.16	1.295	0.1594	1.586		314.05	0.094	3.901	0.0935	3.953
[C_4-mim][BF_4]	303	0.142	7.739	0.1468	8.698		324.15	0.098	3.304	0.0922	5.343
	313	0.146	5.883	0.1487	7.261		334.35	0.101	2.889	0.0909	6.680
	323	0.151	5.097	0.1505	5.830		344.55	0.102	2.876	0.0895	8.462
	333	0.154	3.974	0.1523	4.421	[C_4-mim][Tf_2N]	303.85	0.077	4.934	0.0847	11.678
	343	0.157	3.876	0.1541	3.888		314.05	0.08	6.920	0.0848	10.143
	353	0.161	3.709	0.1560	3.730		324.15	0.081	7.140	0.0848	9.668
	363	0.163	3.210	0.1578	3.959		334.35	0.083	6.173	0.0849	8.365
	373	0.165	3.316	0.1596	4.080		344.55	0.087	5.012	0.0850	6.945
	383	0.172	1.872	0.1614	3.516	[C_6-mim][Tf_2N]	303.85	0.089	8.233	0.0745	9.676
[C_4-mim][PF_6]	303	0.112	5.716	0.1210	7.272		314.05	0.092	6.714	0.0760	8.629
	308	0.114	9.748	0.1213	10.703		324.15	0.095	5.573	0.0775	8.070
	313	0.117	9.421	0.1217	11.001		334.35	0.097	4.282	0.0790	7.706
	318	0.118	9.191	0.1220	10.534		344.55	0.097	3.553	0.0805	7.185
	323	0.122	8.4023	0.1223	9.411	[C_8-mim][Tf_2N]	303.85	0.062	8.056	0.0643	11.895
	328	0.123	8.2045	0.1227	8.986		314.05	0.063	9.171	0.0672	12.153
[C_6-mim][PF_6]	303	0.115	7.575	0.1230	7.714		324.15	0.064	8.744	0.0701	12.262
	308	0.116	7.401	0.1234	7.480		334.35	0.065	8.638	0.0730	12.032
	313	0.117	7.150	0.1114	7.610		344.55	0.071	8.036	0.0759	10.718
	318	0.119	9.348	0.1124	9.518	[C_4-mim][CF_3SO_3]	303.20	0.115	13.726	0.1072	14.825
	323	0.121	6.700	0.1134	7.402		313.30	0.141	8.667	0.1151	9.765
	328	0.122	7.081	0.1145	7.926		323.30	0.147	4.107	0.1230	8.510
	333	0.123	6.712	0.1155	7.705		333.30	0.147	0.898	0.1309	8.439
	338	0.125	6.151	0.1165	7.141		343.20	0.154	6.384	0.1388	10.705

[a] k_{ij} fitted on experimental VLE data. [b] k_{ij} estimated by eq 25. [c] Average absolute deviation in CO_2 mole fraction.

dx.doi.org/10.1021/jp309944t | J. Phys. Chem. B 2012, 116, 14375−14388

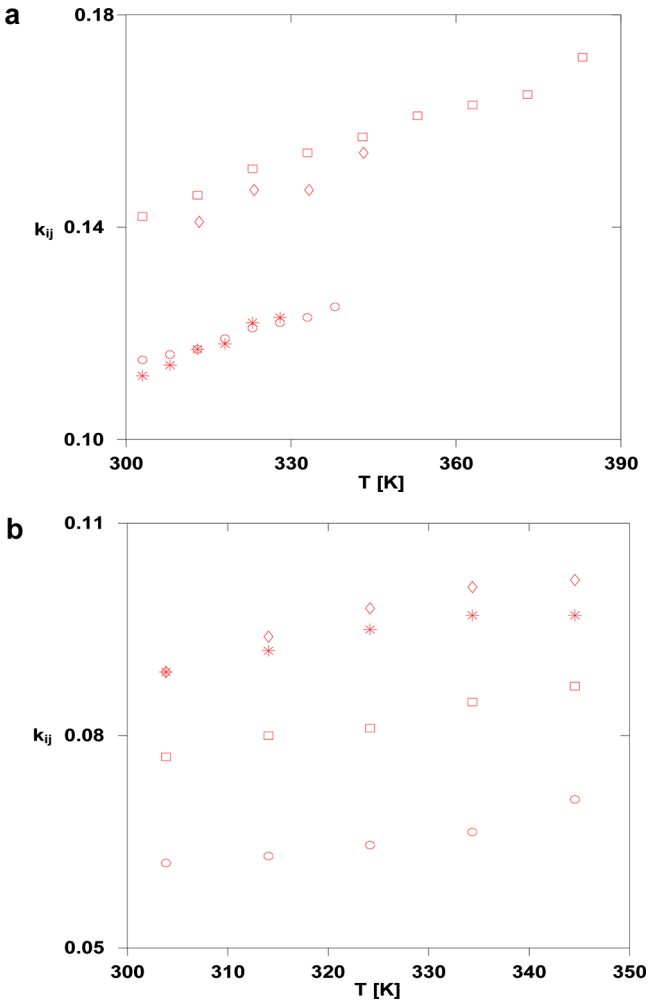

Figure 7. Dependence on temperature of the binary interaction parameter for different ILs mixed with CO_2. (a) [C_4-mim][BF_4] (□), [C_4-mim][PF_6] (*), [C_6-mim][PF_6] (○), and [C_4-mim][CF_3SO_3] (◊); (b) [C_2-mim][Tf_2N] (◊), [C_4-mim][Tf_2N] (□), [C_6-mim]-[Tf_2N] (*), and [C_8-mim][Tf_2N] (○).

Table 6. Parameters Used in Eq 25 to Predict the Binary Interaction Parameter, k_{ij}, for Binary Systems Containing CO_2 and an Imidazolium-Based IL

group	a_i	b_i
[BF_4]	-9.47×10^{-5}	1.98×10^{-1}
[PF_6]	-2.09×10^{-4}	2.06×10^{-1}
[Tf_2N]	-2.66×10^{-4}	1.87×10^{-1}
[CF_3SO_3]	5.14×10^{-4}	-2.82×10^{-2}
[C_2SO_4]	1.98×10^{-4}	8.59×10^{-2}
[C_1SO_4]	-4.32×10^{-5}	1.84×10^{-1}
[DCA]	2.55×10^{-4}	1.11×10^{-1}
[SCN]	-1.62×10^{-4}	2.42×10^{-1}
CH_3/CH_2	-8.81×10^{-1}	-6.72×10^{-1}

absolute deviations on the estimated molar fraction of CO_2 at different temperatures using this approach are presented in Table 5 and can be compared to the results obtained by a direct fit of k_{ij} on experimental VLE data. This table clearly highlights that the proposed eq 25 is very accurate.

We now present and discuss calculations performed with the PC-SAFT EoS to correlate VLE data on systems containing CO_2 and an IL. The interaction parameter k_{ij} was obtained by

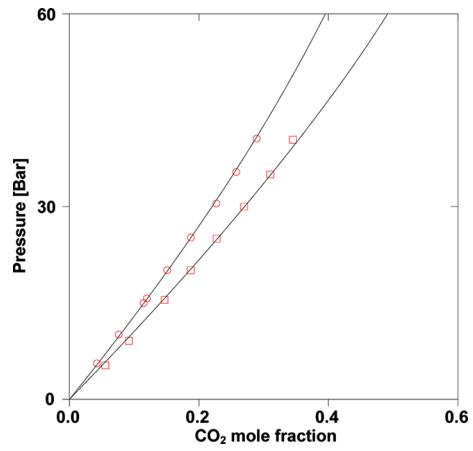

Figure 8. Solubility of CO_2 in [C_2-mim][BF_4] at different temperatures with a temperature-dependent k_{ij} parameter: T = 298.20 K (□) and T = 313.20 K (○). Solid lines represent PC-SAFT calculations.

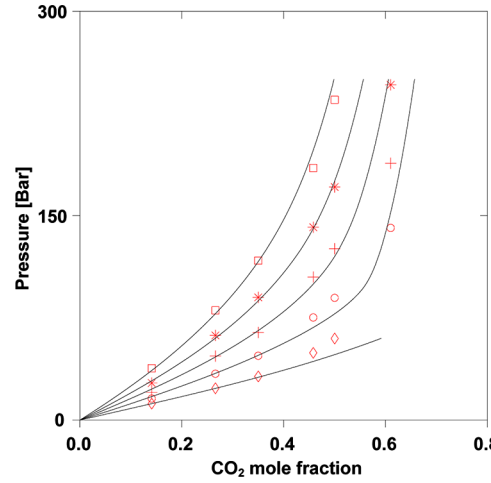

Figure 9. Solubility of CO_2 in [C_4-mim][BF_4] at different temperatures with a temperature-dependent k_{ij} parameter: T = 303 K (◊), T = 323 K (○), T = 343 K (+), T = 363 K (*), and T = 383 K (□). Solid lines represent PC-SAFT calculations.

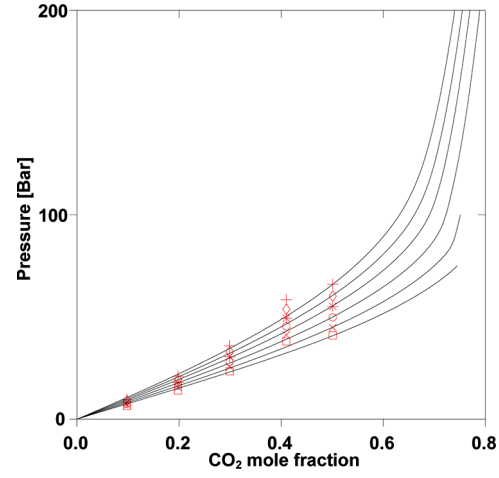

Figure 10. Solubility of CO_2 in [C_6-mim][PF_6] at different temperatures with a temperature-dependent k_{ij} parameter: T = 308 K (□), T = 313 K (×), T = 318 K (○), T = 323 K (*), T = 328 K (◊), and T = 333 K (+). Solid lines represent PC-SAFT calculations.

dx.doi.org/10.1021/jp309944t | J. Phys. Chem. B 2012, 116, 14375−14388

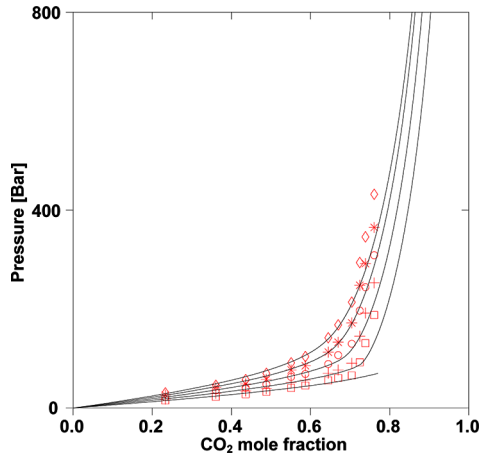

Figure 11. Solubility of CO_2 in $[C_2\text{-mim}][Tf_2N]$ at different temperatures with a temperature-dependent k_{ij} parameter: T = 303.85 K (□), T = 314.05 K (+), T = 324.15 K (○), T = 334.35 K (*), and T = 344.55 K (◊). Solid lines represent PC-SAFT calculations.

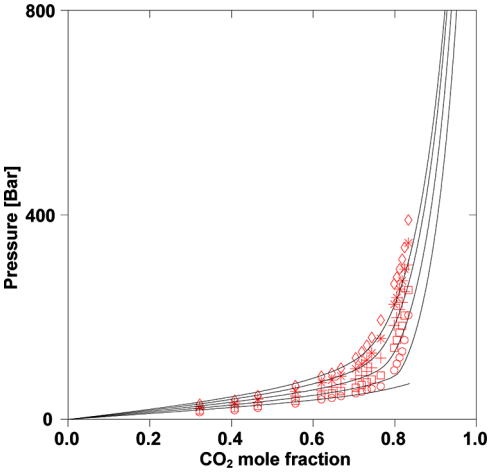

Figure 12. Solubility of CO_2 in $[C_6\text{-mim}][Tf_2N]$ at different temperatures with a temperature-dependent k_{ij} parameter: T = 303.85 K (○), T = 314.05 K (□), T = 324.15 K (+), T = 334.35 K (*), and T = 344.55 K (◊). Solid lines represent PC-SAFT calculations.

fitting to experimental VLE data. First, we studied the mixture $\{[C_2\text{-mim}][BF_4] + CO_2\}$ at two different temperatures: T = 298.20 and 313.20 K. Figure 8 depicts the solubility isotherms obtained for these mixtures as compared to available experimental data.[35] It is striking to see the accuracy of these calculations at low pressures as compared to the experimental data. Within the same family, we studied $\{[C_4\text{-mim}][BF_4] + CO_2\}$ at different temperatures: T = 303, 323, 343, 363, and 383 K. As shown in Figure 9, good agreement between the experimental data[36] and the calculated values can be observed at low pressure. However, a small deviation is observed at high pressure for T = 343 and 363 K.

Phase diagrams of the binary systems $\{[C_6\text{-mim}][PF_6] + CO_2\}$, $\{[C_2\text{-mim}][Tf_2N] + CO_2\}$, and $\{[C_6\text{-mim}][Tf_2N] + CO_2\}$ are represented with average absolute deviations in the CO_2 mole fraction of 7.00%, 3.48%, and 5.67%, respectively. The results presented in Figures 10−12 show that the PC-SAFT model can be used to predict with high accuracy the phase diagrams of these ionic liquids with carbon dioxide.

Finally, Figure 13 shows that the model has difficulty in representing with high accuracy the binary system $\{CO_2 + [C_4\text{-mim}][CF_3SO_3]\}$[37] at 303.20 and 343.20 K, although intermediate temperatures are well represented. Phase diagrams of the binary system $\{[C_4\text{-mim}][CF_3SO_3] + CO_2\}$ are represented with an average absolute deviation in the CO_2 mole fraction of 6.76%.

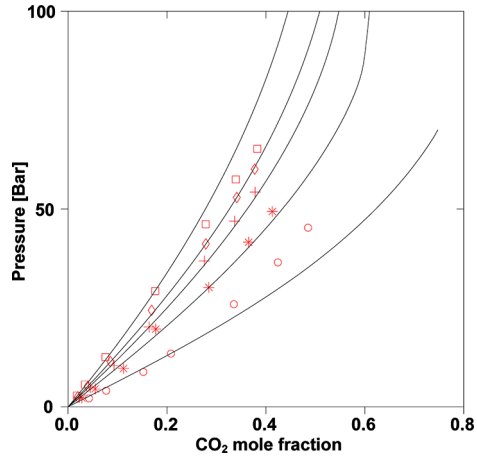

Figure 13. Solubility of CO_2 in $[C_4\text{-mim}][CF_3SO_3]$ at different temperatures with a temperature-dependent k_{ij} parameter: T = 303.20 K (○), T = 313.20 K (*), T = 323.20 K (+), T = 333.20 K (◊), and T = 343.20 K (□). Solid lines represent PC-SAFT calculations.

In general, we notice a higher accuracy at low pressure than at high pressure. As a consequence, the simple model presented here is able to capture the solubility of these mixtures in quantitative agreement with available experimental data. It is also noticeable that the well-known pitfalls of the PC-SAFT EoS[38,39] were not evidenced in this work.

■ CONCLUSIONS

PC-SAFT parameters of pure ILs were estimated from component density data. In a second step, these parameters were simply correlated with the IL molar weight. It is thus possible to estimate m, σ, and ε/k_B for ILs for which no experimental data are available. The interaction parameter k_{ij} is highly temperature-dependent and increases linearly with temperature. The contributions of the anion and the cation to the value of this parameter were investigated. We showed that PC-SAFT EoS is able to reproduce the solubility of CO_2 in imidazolium-based ILs in a wide range of temperatures and pressures.

■ AUTHOR INFORMATION

Corresponding Author

*E-mail: fabrice.mutelet@ensic.inpl-nancy.fr. Tel.: +33 (0) 3.83.17.51.31. Fax: +33 (0)3.83.32.29.75.

Notes

The authors declare no competing financial interest.

■ REFERENCES

(1) Pennline, H. W.; Luebke, D. R.; Jones, K. L.; Myers, C. R.; Morsi, B. I.; Heintz, Y. J.; Ilconich, J. B. *Fuel Process. Technol.* **2008**, *89*, 897−907.
(2) da Silva, E. F.; Svendsen, H. F. *Ind. Eng. Chem. Res.* **2006**, *45*, 2497−2504.
(3) Bello, A.; Idem, R. O. *Ind. Eng. Chem. Res.* **2005**, *44*, 945−969.
(4) Aionicesei, E.; Škerget, M.; Knez, Ž. *J. Chem. Eng. Data* **2008**, *53*, 185−188.

(5) Revelli, A. L.; Mutelet, F.; Jaubert, J. N. *Ind. Eng. Chem. Res.* **2010**, *49*, 3883−3892.
(6) Mutelet, F.; Revelli, A. L.; Jaubert, J. N.; Sprunger, L. M.; Acree, W. E.; Baker, G. A. *J. Chem. Eng. Data* **2010**, *55*, 234−242.
(7) Mutelet, F.; Jaubert, J. N.; Rogalski, M.; Harmand, J.; Sindt, M.; Mieloszynski, J. L. *J. Phys. Chem. B* **2008**, *112*, 3773−3785.
(8) Revelli, A. L.; Mutelet, F.; Turmine, M.; Solimando, R.; Jaubert, J. N. *J. Chem. Eng. Data* **2009**, *54*, 90−101.
(9) Wertheim, M. S. *J. Stat. Phys.* **1984**, *35*, 19−34.
(10) Wertheim, M. S. *J. Stat. Phys.* **1984**, *35*, 35−47.
(11) Wertheim, M. S. *J. Stat. Phys.* **1986**, *42*, 459−476.
(12) Wertheim, M. S. *J. Stat. Phys.* **1986**, *42*, 477−492.
(13) Chapman, W. G.; Jackson, G.; Gubbins, K. E. *Mol. Phys.* **1988**, *65*, 1057−1079.
(14) Chapman, W. G.; Gubbins, K. E.; Jackson, G.; Radosz, M. *Ind. Eng. Chem. Res.* **1990**, *29*, 1709−1721.
(15) Huang, S. H.; Radosz, M. *Ind. Eng. Chem. Res.* **1990**, *29*, 2284−2294.
(16) Fu, Y. H.; Sandler, S. I. *Ind. Eng. Chem. Res.* **1995**, *34*, 1897−1909.
(17) Garcia-Lisbona, M. N.; Galindo, A.; Jackson, G.; Burgess, A. N. *J. Am. Chem. Soc.* **1998**, *120*, 4191−4199.
(18) GilVillegas, A.; Galindo, A.; Whitehead, P. J.; Mills, S. J.; Jackson, G.; Burgess, A. N. *J. Chem. Phys.* **1997**, *106*, 4168−4186.
(19) Pamies, J. C.; Vega, L. F. *Ind. Eng. Chem. Res.* **2001**, *40*, 2532−2543.
(20) Blas, F. J.; Vega, L. F. *Mol. Phys.* **1997**, *92*, 135−150.
(21) Gross, J.; Sadowski, G. *Ind. Eng. Chem. Res.* **2001**, *40*, 1244−1260.
(22) Llovell, F.; Valente, E.; Vilaseca, O.; Vega, L. F. *J. Phys. Chem. B* **2011**, *115*, 4387−4398.
(23) Karakatsani, E. K.; Economou, I. G. *J. Phys. Chem. B* **2006**, *110*, 9252−9261.
(24) Karakatsani, E. K.; Kontogeorgis, G. M.; Economou, I. G. *Ind. Eng. Chem. Res.* **2006**, *45*, 6063−6074.
(25) Kroon, M. C.; Karakatsani, E. K.; Economou, I. G.; Witkamp, G.-J.; Peters, C. J. *J. Phys. Chem. B* **2006**, *110*, 9262−9269.
(26) Karakatsani, E. K.; Economou, L. G.; Kroon, M. C.; Peters, C. J.; Witkamp, G. J. *J. Phys. Chem. C* **2007**, *111*, 15487−15492.
(27) Paduszynski, K.; Domanska, U. *J. Phys. Chem. B* **2011**, *115*, 12537−12548.
(28) Baker, J. A.; Henderson, D. *J. Chem. Phys.* **1967**, *47*, 2856−2861.
(29) Baker, J. A.; Henderson, D. *J. Chem. Phys.* **1967**, *47*, 4714−4721.
(30) Huang, S. H.; Radosz, M. *Ind. Eng. Chem. Res.* **1991**, *30*, 1994−2005.
(31) Wolbach, J. P.; Sandler, S. I. *Ind. Eng. Chem. Res.* **1998**, *37*, 2917−2928.
(32) Pamies, J. C. Ph.D. Thesis, Universitat Rovira i Virgili, Tarragona, Spain, 2003.
(33) Andreu, J. S.; Vega, L. F. *J. Phys. Chem. C* **2007**, *111*, 16028−16034.
(34) Sanmamed, Y. A.; Gonzalez-Salgado, D.; Troncoso, J.; Cerdeirina, C. A.; Romani, L. *Fluid Phase Equilib.* **2007**, *252*, 96−102.
(35) Lei, Z.; Yuan, J.; Zhu, J. *J. Chem. Eng. Data* **2010**, *55*, 4190−4194.
(36) Revelli, A.-L.; Mutelet, F.; Jaubert, J.-N. *J. Phys. Chem. B* **2010**, *114*, 12908−12913.
(37) Soriano, A. N.; Doma, B. T., Jr.; Li, M.-H. *J. Taiwan Inst. Chem. Eng.* **2009**, *40*, 387−393.
(38) Privat, R.; Gani, R.; Jaubert, J.-N. *Fluid Phase Equilib.* **2010**, *295*, 76−92.
(39) Privat, R.; Conte, E.; Jaubert, J. N.; Gani, R. *Fluid Phase Equilib.* **2012**, *318*, 61−76.
(40) Klomfar, J.; Součková, M.; Pátek, J. *Fluid Phase Equilib.* **2009**, *282*, 31−37.
(41) Stoppa, A.; Zech, O.; Kunz, W.; Buchner, R. *J. Chem. Eng. Data* **2010**, *55*, 1768−1773.
(42) Seddon, K. R.; Stark, A.; Torres, M.-J. *ACS Symp. Ser.* **2002**, *819*, 34−49.
(43) Navia, P.; Troncoso, J.; Romani, L. *J. Chem. Eng. Data* **2007**, *52*, 1369−1374.
(44) Shiflett, M. B.; Yokozeki, A. *J. Chem. Eng. Data* **2007**, *52*, 1302−1306.
(45) Schreiner, C.; Zugmann, S.; Hartl, R.; Gores, H. J. *J. Chem. Eng. Data* **2010**, *55*, 1784−1788.
(46) Stoppa, A.; Hunger, J.; Buchner, R. *J. Chem. Eng. Data* **2009**, *54*, 472−479.
(47) Nishida, T.; Tashiro, Y.; Yamamoto, M. *J. Fluorine Chem.* **2003**, *120*, 135−141.
(48) Huo, Y.; Xia, S.; Ma, P. *J. Chem. Eng. Data* **2008**, *53*, 2535−2539.
(49) Huo, Y.; Xia, S. Q.; Ma, P. S. *J. Chem. Eng. Data* **2007**, *52*, 2077−2082.
(50) Vakili-Nezhaad, G.; Vatani, M.; Asghari, M.; Ashour, I. *J. Chem. Thermodyn.* **2012**, *54*, 148−154.
(51) Fredlake, C. P.; Crosthwaite, J. M.; Hert, D. G.; Aki, S. N. V. K.; Brennecke, J. F. *J. Chem. Eng. Data* **2004**, *49*, 954−964.
(52) Zhou, Q.; Wang, L. S.; Chen, H. P. *J. Chem. Eng. Data* **2006**, *51*, 905−908.
(53) Jacquemin, J.; Husson, P.; Padua, A. A. H.; Majer, V. *Green Chem.* **2006**, *8*, 172−180.
(54) Tokuda, H.; Tsuzuki, S.; Susan, M. A. B. H.; Hayamizu, K.; Watanabe, M. *J. Phys. Chem. B* **2006**, *110*, 19593−19600.
(55) Iglesias-Otero, M. A.; Troncoso, J.; Carballo, E.; Romani, L. *J. Solution Chem.* **2007**, *36*, 1219−1230.
(56) Harris, K. R.; Kanakubo, M.; Woolf, L. A. *J. Chem. Eng. Data* **2007**, *52*, 2425−2430.
(57) Kumar, A. *J. Solution Chem.* **2008**, *37*, 203−214.
(58) Garcia-Miaja, G.; Troncoso, J.; Romani, L. *Fluid Phase Equilib.* **2008**, *274*, 59−67.
(59) Qi, F.; Wang, H. J. *J. Chem. Thermodyn.* **2009**, *41*, 265−272.
(60) Gao, H. Y.; Qi, F.; Wang, H. J. *J. Chem. Thermodyn.* **2009**, *41*, 888−892.
(61) Sanchez, L. G.; Espel, J. R.; Onink, F.; Meindersma, G. W.; de Haan, A. B. *J. Chem. Eng. Data* **2009**, *54*, 2803−2812.
(62) Garcia-Miaja, G.; Troncoso, J.; Romani, L. *J. Chem. Thermodyn.* **2009**, *41*, 334−341.
(63) Soriano, A. N.; Doma, B. T., Jr.; Li, M.-H. *J. Chem. Thermodyn.* **2009**, *41*, 301−307.
(64) Li, Y.; Ye, H.; Zeng, P. L.; Qi, F. *J. Solution Chem.* **2010**, *39*, 219−230.
(65) Harris, K. R.; Kanakubo, M.; Woolf, L. A. *J. Chem. Eng. Data* **2006**, *51*, 1161−1167.
(66) Gardas, R. L.; Freire, M. G.; Caryalho, P. J.; Marrucho, I. M.; Fonseca, I. M. A.; Ferreira, A. G. M.; Coutinho, J. A. P. *J. Chem. Eng. Data* **2007**, *52*, 80−88.
(67) Gu, Z. Y.; Brennecke, J. F. *J. Chem. Eng. Data* **2002**, *47*, 339−345.
(68) Kabo, G. J.; Blokhin, A. V.; Paulechka, Y. U.; Kabo, A. G.; Shymanovich, M. P.; Magee, J. W. *J. Chem. Eng. Data* **2004**, *49*, 453−461.
(69) Kumelan, J.; Kamps, A. P. S.; Tuma, D.; Maurer, G. *Fluid Phase Equilib.* **2005**, *228*, 207−211.
(70) Harris, K. R.; Woolf, L. A.; Kanakubo, M. *J. Chem. Eng. Data* **2005**, *50*, 1777−1782.
(71) Zafarani-Moattar, M. T.; Shekaari, H. *J. Chem. Eng. Data* **2005**, *50*, 1694−1699.
(72) Jacquemin, J.; Husson, P.; Majer, V.; Gomes, M. F. C. *Fluid Phase Equilib.* **2006**, *240*, 87−95.
(73) Troncoso, J.; Cerdeirina, C. A.; Sanmamed, Y. A.; Romani, L.; Rebelo, L. P. N. *J. Chem. Eng. Data* **2006**, *51*, 1856−1859.
(74) Jacquemin, J.; Husson, P.; Mayer, V.; Cibulka, I. b. *J. Chem. Eng. Data* **2007**, *52*, 2204−2211.
(75) Pereiro, A. B.; Legido, J. L.; Rodriguez, A. *J. Chem. Thermodyn.* **2007**, *39*, 1168−1175.
(76) Pereiro, A. B.; Rodriguez, A. *J. Chem. Thermodyn.* **2007**, *39*, 978−989.

(77) Pereiro, A. B.; Rodriguez, A. *J. Chem. Eng. Data* **2007**, *52*, 600−608.
(78) Kumar, A.; Singh, T.; Gardas, R. L.; Coutinho, J. A. P. *J. Chem. Thermodyn.* **2008**, *40*, 32−39.
(79) Fan, W.; Zhou, Q.; Sun, J.; Zhang, S. J. *J. Chem. Eng. Data* **2009**, *54*, 2307−2311.
(80) Zech, O.; Stoppa, A.; Buchner, R.; Kunz, W. *J. Chem. Eng. Data* **2010**, *55*, 1774−1778.
(81) Singh, T.; Kumar, A. *J. Mol. Liq.* **2010**, *153*, 117−123.
(82) Muhammad, A.; Mutalib, M. I. A.; Wilfred, C. D.; Murugesan, T.; Shafeeq, A. *J. Chem. Thermodyn.* **2008**, *40*, 1433−1438.
(83) Pereiro, A. B.; Tojo, E.; Rodriguez, A.; Canosa, J.; Tojo, J. *J. Chem. Thermodyn.* **2006**, *38*, 651−661.
(84) Harris, K. R.; Kanakubo, M.; Woolf, L. A. *J. Chem. Eng. Data* **2007**, *52*, 1080−1085.
(85) Tomida, D.; Kenmochi, S.; Tsukada, T.; Qiao, K.; Yokoyama, C. *Int. J. Thermophys.* **2007**, *28*, 1147−1160.
(86) Taguchi, R.; Machida, H.; Sato, Y.; Smith, R. L. *J. Chem. Eng. Data* **2009**, *54*, 22−27.
(87) Tomida, D.; Kumagai, A.; Kenmochi, S.; Qiao, K.; Yokoyama, C. *J. Chem. Eng. Data* **2007**, *52*, 577−579.
(88) Tariq, M.; Serro, A. P.; Mata, J. L.; Saramago, B.; Esperança, J. M. S. S.; Lopes, J. N. C.; Rebelo, L. P. N. *Fluid Phase Equilib.* **2010**, *294*, 131−138.
(89) Krummen, M.; Wasserscheid, P.; Gmehling, J. *J. Chem. Eng. Data* **2002**, *47*, 1411−1417.
(90) Tokuda, H.; Hayamizu, K.; Ishii, K.; Susan, M.; Watanabe, M. *J. Phys. Chem. B* **2005**, *109*, 6103−6110.
(91) Jacquemin, J.; Husson, P.; Majer, V.; Gomes, M. F. C. *J. Solution Chem.* **2007**, *36*, 967−979.
(92) Gardas, R. L.; Freire, M. G.; Carvalho, P. J.; Marrucho, I. M.; Fonseca, I. M. A.; Ferreira, A. G. M.; Coutinho, J. A. P. *J. Chem. Eng. Data* **2007**, *52*, 1881−1888.
(93) Wandschneider, A.; Lehmann, J. K.; Heintz, A. *J. Chem. Eng. Data* **2008**, *53*, 596−599.
(94) Esperanca, J.; Visak, Z. P.; Plechkova, N. V.; Seddon, K. R.; Guedes, H. J. R.; Rebelo, L. P. N. *J. Chem. Eng. Data* **2006**, *51*, 2009−2015.
(95) de Azevedo, R. G.; Esperanca, J.; Szydlowski, J.; Visak, Z. P.; Pires, P. F.; Guedes, H. J. R.; Rebelo, L. P. N. *J. Chem. Thermodyn.* **2005**, *37*, 888−899.
(96) Palgunadi, J.; Kang, J. E.; Nguyen, D. Q.; Kim, J. H.; Min, B. K.; Lee, S. D.; Kim, H.; Kim, H. S. *Thermochim. Acta* **2009**, *494*, 94−98.
(97) Kato, R.; Gmehling, J. *J. Chem. Thermodyn.* **2005**, *37*, 603−619.
(98) Kumelan, J.; Kamps, I. P. S.; Tuma, D.; Maurer, G. *J. Chem. Thermodyn.* **2006**, *38*, 1396−1401.
(99) Widegren, J. A.; Magee, J. W. *J. Chem. Eng. Data* **2007**, *52*, 2331−2338.
(100) Kandil, M. E.; Marsh, K. N.; Goodwin, A. R. H. *J. Chem. Eng. Data* **2007**, *52*, 2382−2387.
(101) Ahosseini, A.; Sensenich, B.; Weatherley, L. R.; Scurto, A. M. *J. Chem. Eng. Data* **2010**, *55*, 1611−1617.
(102) Esperanca, J.; Guedes, H. J. R.; Lopes, J. N. C.; Rebelo, L. P. N. *J. Chem. Eng. Data* **2008**, *53*, 867−870.
(103) Zaitsau, D. H.; Kabo, G. J.; Strechan, A. A.; Paulechka, Y. U.; Tschersich, A.; Verevkin, S. P.; Heintz, A. *J. Phys. Chem. A* **2006**, *110*, 7303−7306.
(104) Alonso, L.; Arce, A.; Francisco, M.; Soto, A. *J. Chem. Thermodyn.* **2008**, *40*, 265−270.
(105) Freire, M. G.; Teles, A. R. R.; Rocha, M. A. A.; Schroder, B.; Neves, C.; Carvalho, P. J.; Evtuguin, D. V.; Santos, L.; Coutinho, J. A. P. *J. Chem. Eng. Data* **2011**, *56*, 4813−4822.
(106) Domańska, U.; Laskowska, M. *J. Chem. Eng. Data* **2009**, *54*, 2113−2119.
(107) Domańska, U.; Królikowska, M. *J. Chem. Eng. Data* **2010**, *55*, 2994−3004.
(108) Vercher, E.; Orchillés, A. V.; Miguel, P. J.; Martíhez-Andreu, A. *J. Chem. Eng. Data* **2007**, *52*, 1468−1482.
(109) García-Miaja, G.; Troncoso, J.; Romaní, L. *J. Chem. Thermodyn.* **2009**, *41*, 161−166.
(110) Gardas, R. L.; Costa, H. F.; Freire, M. G.; Carvalho, P. J.; Marrucho, I. M.; Fonseca, I. M. A.; Ferreira, A. G.; Coutinho, J. A. P. *J. Chem. Eng. Data* **2008**, *53*, 805−811.
(111) Wong, C.-L.; Soriano, A. N.; Li, M.-H. *Fluid Phase Equilib.* **2008**, *271*, 43−52.
(112) Rodríguez, H.; Brennecke, J. F. *J. Chem. Eng. Data* **2006**, *51*, 2145−2155.
(113) Ge, M. L.; Zhao, R. S.; Yi, Y. F.; Zhang, Q.; Wang, L. S. *J. Chem. Eng. Data* **2008**, *53*, 2408−2411.
(114) Ficke, L. E.; Novak, R. R.; Brennecke, J. F. *J. Chem. Eng. Data* **2010**, *55*, 4946−4950.
(115) Nebig, S.; Gmehling, J. *Fluid Phase Equilib.* **2010**, *294*, 206−212.
(116) Mokhtarani, B.; Sharifi, A.; Mortaheb, H. R.; Mirzaei, M.; Mafi, M.; Sadeghian, F. *J. Chem. Thermodyn.* **2009**, *41*, 1432−1438.
(117) Blanchard, L. A.; Gu, Z.; Brennecke, J. F. *J. Phys. Chem. B* **2001**, *105*, 2437−2444.
(118) Klomfar, J.; Souckova, M.; Patek, J. *J. Chem. Eng. Data* **2011**, *56*, 3454−3462.
(119) Carvalho, P. J.; Regueira, T.; Santos, L. M. N. B. F.; Fernandez, J.; Coutinho, J. A. P. *J. Chem. Eng. Data* **2010**, *55*, 645−652.
(120) Seoane, R. G.; Corderi, S.; Gomez, E.; Calvar, N.; Gonzalez, E. J.; Macedo, E. A.; Dominguez, A. *Ind. Eng. Chem. Res.* **2012**, *51*, 2492−2504.
(121) Singh, T.; Kumar, A. *J. Solution Chem.* **2009**, *38*, 1043−1053.
(122) Kumelan, J.; Kamps, A. P. S.; Tuma, D.; Maurer, G. *J. Chem. Eng. Data* **2006**, *51*, 1802−1807.
(123) Pereiro, A. B.; Verdia, P.; Tojo, E.; Rodriguez, A. *J. Chem. Eng. Data* **2007**, *52*, 377−380.
(124) Gonzalez, B.; Calvar, N.; Gomez, E.; Dominguez, A. *J. Chem. Thermodyn.* **2008**, *40*, 1274−1281.
(125) Fernandez, A.; Garcia, J.; Torrecilla, J. S.; Oliet, M.; Rodriguez, F. *J. Chem. Eng. Data* **2008**, *53*, 1518−1522.
(126) Gómez, E.; González, B.; Calvar, N.; Tojo, E.; Domínguez, Á. *J. Chem. Eng. Data* **2006**, *51*, 2096−2102.
(127) Yang, J. Z.; Lu, X. M.; Gui, J. S.; Xu, W. G. *Green Chem.* **2004**, *6*, 541−543.
(128) Yang, H. Z.; Lu, X. M.; Gui, J. S.; Xu, W. G.; Li, H. W. *J. Chem. Thermodyn.* **2005**, *37*, 1250−1255.
(129) Gonzalez, E. J.; Gonzalez, B.; Calvar, N.; Dominguez, A. *J. Chem. Eng. Data* **2007**, *52*, 1641−1648.
(130) Hofman, T.; Goldon, A.; Nevines, A.; Letcher, T. M. *J. Chem. Thermodyn.* **2008**, *40*, 580−591.
(131) Tome, L. I. N.; Carvalho, P. J.; Freire, M. G.; Marrucho, I. M.; Fonseca, I. M. A.; Ferreira, A. G. M.; Coutinho, J. A. P.; Gardas, R. L. *J. Chem. Eng. Data* **2008**, *53*, 1914−1921.
(132) Matkowska, D.; Goldon, A.; Hofman, T. *J. Chem. Eng. Data* **2010**, *55*, 685−693.
(133) Machida, H.; Taguchi, R.; Sato, Y.; Smith, R. L., Jr. *J. Chem. Eng. Data* **2011**, *56*, 923−928.
(134) Govinda, V.; Attri, P.; Venkatesu, P.; Venkateswarlu, P. *Fluid Phase Equilib.* **2011**, *304*, 35−43.
(135) Huddleston, J. G.; Visser, A. E.; Reichert, W. M.; Willauer, H. D.; Broker, G. A.; Rogers, R. D. *Green Chem.* **2001**, *3*, 156−164.
(136) Gomez, E.; Gonzalez, B.; Dominguez, A.; Tojo, E.; Tojo, J. *J. Chem. Eng. Data* **2006**, *51*, 696−701.
(137) Gonzalez, E. J.; Alonso, L.; Dominguez, A. *J. Chem. Eng. Data* **2006**, *51*, 1446−1452.
(138) David, W.; Letcher, T. M.; Ramjugernath, D.; Raal, J. D. *J. Chem. Thermodyn.* **2003**, *35*, 1335−1341.
(139) Fröba, A. P.; Rausch, M. H.; Krzeminski, K.; Assenbaum, D.; Wasserscheid, P.; Leipertz, A. *Int. J. Thermophys.* **2010**, *31*, 2059−2077.
(140) Quijada-Maldonado, E.; van der Boogaart, S.; Lijbers, J. H.; Meindersma, G. W.; de Haan, A. B. *J. Chem. Thermodyn.* **2012**, *51*, 51−58.

(141) Shiflett, M. B.; Kasprzak, D. J.; Junk, C. P.; Yokozeki, A. *J. Chem. Thermodyn.* **2008**, *40*, 25−31.
(142) Bogolitsyn, K. G.; Skrebets, T. E.; Makhova, T. A. *Russ. J. Gen. Chem.* **2009**, *79*, 125−128.
(143) Li, J.-G.; Hu, Y.-F.; Sun, S.-F.; Liu, Y.-S.; Liu, Z.-C. *J. Chem. Thermodyn.* **2010**, *42*, 904−908.
(144) Rocha, M. A. A.; Lima, C.; Gomes, L. R.; Schroder, B.; Coutinho, J. A. P.; Marrucho, I. M.; Esperanca, J.; Rebelo, L. P. N.; Shimizu, K.; Lopes, J. N. C.; Santos, L. *J. Phys. Chem. B* **2011**, *115*, 10919−10926.
(145) Paduszynski, K.; Domanska, U. *J. Phys. Chem. B* **2011**, *116*, 5002−5018.